Soft Matter

PAPER

View Article Online
View Journal | View Issue

Cite this: *Soft Matter*, 2023, **19**, 9173

Dehydration of biological membranes in a non-condensing environment

G. Hernández-Galván and H. Mercado-Uribe *

Received 4th September 2023,
Accepted 10th November 2023

DOI: 10.1039/d3sm01181j

rsc.li/soft-matter-journal

The study of the dehydration process in a cell membrane allows a better understanding of how water is bound to it. While in prior studies, cell dehydration was commonly analyzed under osmotic stress conditions, in the present work, we focus on the dehydration driven by evaporation in a restricted condensing environment. Using a thermogravimetry method, we studied the dehydration of *Escherichia coli* through isothermal evaporation in the presence of a gas flux. To figure out the loss of mass in this situation, we first evaluated the dynamics of water evaporation of a suspension of multilamellar liposomes. We found that the evaporation of liposomal suspensions composed of individual lipids is constant, although slightly restricted by the presence of liposomes, while the evaporation of liposomal suspensions composed of a mixture of different lipids follows an exponential decay. This is explained considering that the internal pressure at the air–water interface is proportional to the amount of bound water. The evaporation of water from a biomass sample follows this latter behaviour.

1 Introduction

Water is not only a universal solvent. Although generally not considered in biological processes, water is an active molecule with an important role in the structure and function of cells. In this context, cells have developed mechanisms to preserve their morphology and size when the extracellular surrounding is disturbed, and hydration is threatened. It is well-known that the high osmotic pressure in the cytoplasm is regulated by a high hydraulic pressure through the cell membrane. Water flows across the semipermeable membrane minimizing Gibbs energy, from an area of lower solute concentration to one of high concentration, until the solution concentration in both areas is the same. This aligns with an increase of the entropy change, which is achieved by solute solvation.[1] As water flows across the membrane, the solutes gain disorder, entropy increases, and the system moves to energetic equilibrium.

A high osmotic pressure is not the only cause by which water flows from the inside of a cell. Water can also escape by a reduction of vapour pressure. The kinetics of this phenomenon can be studied by analyzing the interface of a hydrated sample, for example, a cell culture. In a typical situation, air just above the sample is saturated with water vapour. Then, when a liquid molecule is released from the sample interface, it can be reflected back by the vapour phase, or it can be substituted by another one. In other words, the existence of gas in the environment influences the evaporation kinetics. In an equilibrium situation, such conversion between vapour and liquid molecules results in a final flow rate equal to zero.[2,3]

It is well-known that dehydration in cells causes several consequences, in particular, changes in the fluidity of the membrane due to the increase of the packing density, and a boost of reactive oxygen species (ROS) that leads to lipid peroxidation, denaturation of proteins, and eventually death.[4–6] This has been studied in different organisms. For instance, *Acinetobacter baumannii* shows a phase transition of lipopolysaccharides (LPSs) and phospholipids during dehydration of the outer membrane. They pass from a liquid crystalline phase to a gel phase. *A. baumannii* is a multi-drug resistant bacterium that causes severe contamination in intensive care units due to its developed exceptional mechanism of protection against dehydration.[7]

Understanding the mechanisms involved in membrane dehydration is a big challenge. While in prior studies, dehydration processes in cells were commonly analyzed under osmotic stress conditions, in the present work, we focus on dehydration through evaporation. We study by thermogravimetry the dehydration of a *E. coli* membrane through isothermal evaporation with a gas flux. The flux guaranties that only evaporation is present (zero condensation).

Due to the fact that the lipid bilayer is the backbone of the cell and the lipid composition determines the fluidity of membranes, it is common to approach its study using artificial models, and one of them is the liposome. It is composed of two layers of lipids, which are amphiphilic molecules consisting of a polar head-group and a hydrophobic tail with two fatty acid chains.[8]

CINVESTAV-Monterrey, PIIT, Apodaca, Nuevo León, 66600, Mexico.
E-mail: hmercado@cinvestav.mx

The properties of lipids depend on the length of the tail, head-group type, chemical structure and polarity.[8,9] Lipid membranes do not form in the absence of water, for its presence guarantees their assembly and thermodynamic stability.[10] Interestingly, water molecules exhibit distinctive thermodynamic properties depending on their location in the membrane.

Molecular dynamics simulations show that there are around 10 water molecules in the interphase of the membrane lipid of which up to three of them are tightly bound to lipids, where 40 kJ mol^{-1} (enthalpy of vaporization at 25 °C) is necessary for breaking the hydrogen bonds. The interphase is a region contained between two planes (or interfaces): the internal plane at the carbonyl group and the external slipping plane in contact with the aqueous phase. Water inside this interphase contributes to around 40% of the total bilayer thickness.[10–14]

Hydration molecules are located on the head-groups with free grades restricted most of the time, and their thermodynamic properties contrast with respect to bulk water.[12,15,16] The latter is basically unaffected by the surfaces of the biomolecules, usually called "free" water.

The aim of this article is to report experimental results obtained from thermogravimetry in the study of the dehydration process of biomembrane models as a first approximation of a *E. coli* membrane, which was also considered.

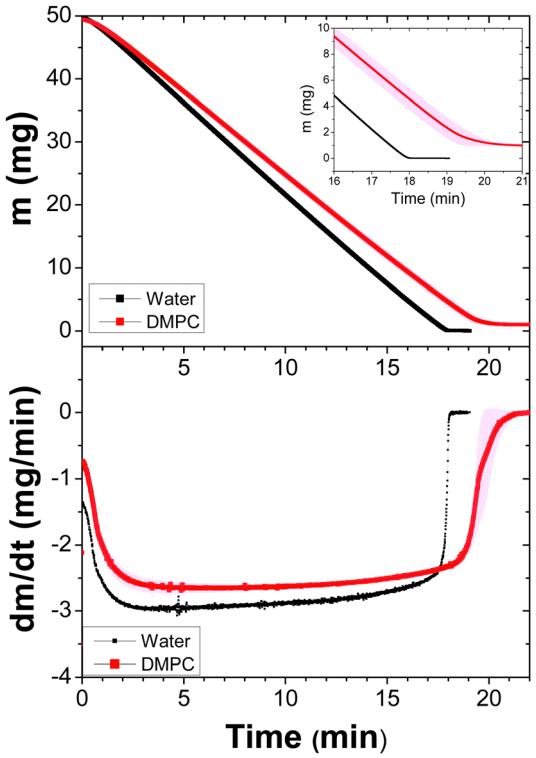

Fig. 1 Dynamics of the dehydration process of DPPC liposomes (50 μL) at a concentration of 2%. Three samples were measured at 37 °C with a constant helium flux (60 mL min^{-1}). The average and standard deviations (due to the fact that the measurements provide many data, the errors bars form a band) are shown. Top: Weight loss emphasizing the last few minutes (inset). Bottom: The first derivative of the data as a function of time. A sample of Milli-Q water is plotted as the reference.

2 Materials and methods

2.1 Liposome preparation

We used the following lyophilized lipids for the preparation of liposomes: 1,2-dimyristoyl-*sn-glycero*-3-phosphocholine, 14C (DMPC), and 1,2-dipalmitoyl-*sn-glycero*-3-phosphocholine, 16C (DPPC), purchased from Avanti Polar Lipids. Each sample of lipid power was weighed using an analytical balance (Explorer EX224, OHAUS) to prepare an aqueous suspension of multilamellar vesicles (MLVs). The weighed lipid (3 mg) was hydrated with 150 μL of deionized water (Milli-Q) to obtain a final concentration of 2%. The sample was stirred with a magnetic bar at 280 rpm for 1 h and thermalized above the melting transition of the lipid. The liposome suspension was stored in an amber jar until it was used.

2.2 Bacterial culture preparation

Escherichia coli K12-MG-1655 was stored in a mixture of Luria-Bertani (LB) broth and glycerol (20%). For the experiments, cultures were prepared by inoculating the colonies (1 mL) into a flask containing 25 mL of the LB medium and left for incubation at 37 °C and 180 rpm. Three samples were taken every 15 minutes for measuring their optical density (OD) using a spectrophotometer (Multiskan GO, Thermo Scientific). The samples were used when the OD was around 0.5.

2.3 Dehydration

In order to analyze the evaporation process of biological membranes, we studied two types of samples: a membrane model consisting of different liposomes and *E. coli* biomass. For the model, we used two lipids to form three different multilamellar liposomes: DMPC (whose transition temperature, T_m, is 23 °C), DPPC (T_m = 41 °C) and DMPC–DPPC mixture (50 : 50). DMPC and DPPC are lipids composed of chains of 14 and 16 carbon atoms, respectively. For the biomass, we used *E. coli* bacteria. The inoculated medium was poured into a 15 mL centrifuge tube and centrifuged at 4500 rpm for 10 min to obtain a pellet. This was repeated twice to obtain a concentrated biomass. The measurements were carried out using a Q500 Thermogravimetric Analyzer (TGA, TA Instruments) with a helium flux (60 mL min^{-1}). Thermogravimetry measurements were performed at different temperatures above the phase transitions of the liposomes (37 °C for DMPC, 47 °C for DPPC and 37 °C, for DMPC–DPPC) until the samples were completely dried. Biomass experiments were carried out at 37 °C. We made mass loss evaluations of pure water under the same conditions as a reference.

3 Results and discussion

The idea of using lipids of different sizes to form liposomes and assess their effects in the evaporation of suspensions has some precedents. Some authors have reported that water permeability is affected when the size, charge of head-groups and chain

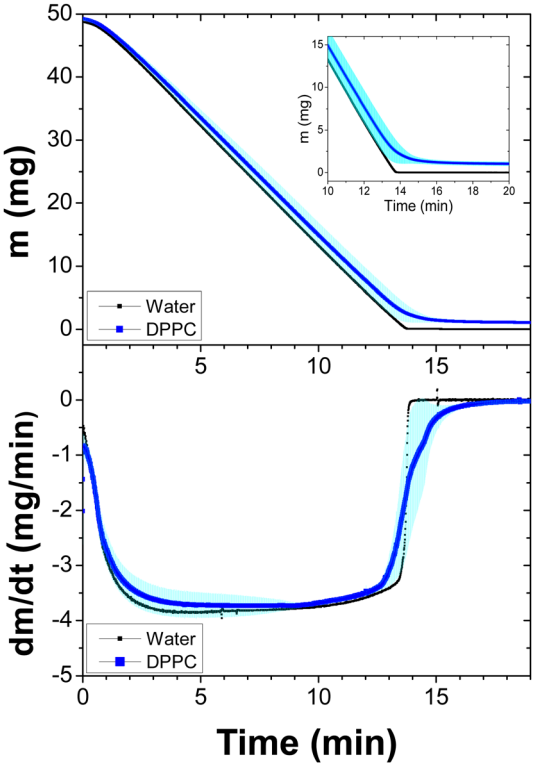

Fig. 2 Dynamics of the dehydration process of DPPC liposomes (50 μL) at a concentration of 2%. Three samples were measured at 47 °C with a constant helium flux (60 mL min^{-1}). The average and standard deviations (due to the fact that the measurements provide many data, the errors bars form a band) are shown. Top: Weight loss emphasizing the last few minutes (inset). Bottom: The first derivative of the data as a function of time. A sample of Milli-Q water is plotted as the reference.

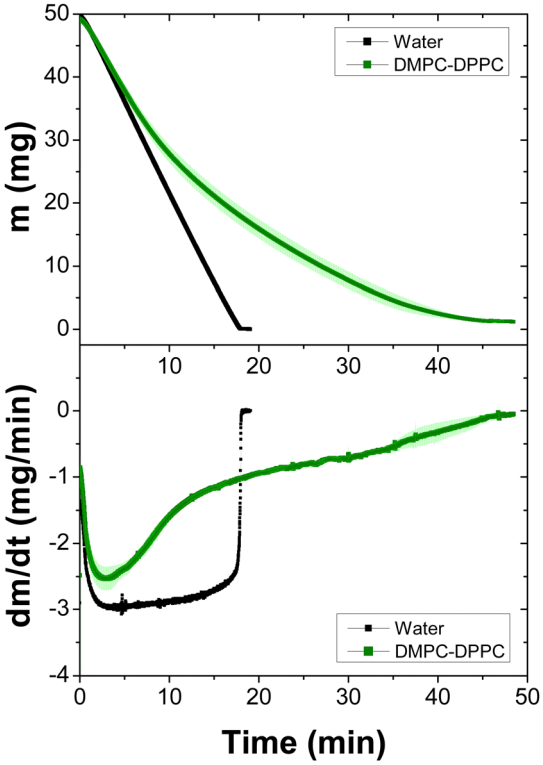

Fig. 3 Dynamics of the dehydration process of a DMPC–DPPC (50 : 50) mixture (50 μL) at a concentration of 2%. Three samples were measured at 37 °C with a constant helium flux (60 mL min^{-1}). The average and standard deviations (due to the fact that the measurements provide many data, the errors bars form a band) are shown. Top: Weight loss as a function of time. Bottom: The first derivative of the data as a function of time. A sample of Milli-Q water is plotted as the reference.

lengths are modified, whereas the bilayer thickness has poor influence.[17,18] In this context, we analyzed the evaporation of liposomal suspensions made of DMPC and DPPC lipids, which are different only by the length of their tails.

Evaporation measurements were performed using a helium flux by isothermal assays at temperatures above the lipid phase transition. The isotherms and first derivatives of the three liposomal suspensions were plotted for each case. Fig. 1 shows the case for the suspensions of DMPC liposomes at 37 °C by triplicate and compared to a control sample (pure water). Note that the stabilization of temperature occurs during the first two minutes of the measurements. Subsequently, the mass loss is constant for both cases, although pure water evaporates faster. Indeed, the difference in the slopes means that liposomes affect the evaporation of water molecules. At the end of the process, when free water has almost vanished, the mass loss slows down. This can be appreciated in the inset of the figure (top) and the first derivative (bottom).

Next, we proceeded in a similar way for the DPPC liposome suspensions, which were measured at 47 °C, see Fig. 2. As expected, since the temperature is higher, the evaporation process is faster than that in DMPC suspensions. However, just before the samples completely dry out, the evaporation again slows down. See the inset in the top panel and the first derivative at the bottom panel. It is clear from the above results that Fig. 1 and 2 show that the evaporation dynamics of drops from these suspensions are very similar, despite the fact that evaporation temperatures are different.

Fig. 3 depicts the mass loss and first derivative of the hybrid sample measured at 37 °C. These results are completely contrasting compared to suspensions of pure liposomes, indicating that most of their released water molecules belong to the bulk. In this case, most of the water molecules composed the hydration shell, giving rise to restricted evaporation. This is more evident in the first derivative. Variations in the tail size affect the thickness of the hydrophobic region and also how the choline region is hydrated. From molecular dynamic simulations, it has been concluded that the area per lipid for DPPC is greater than that for DMPC, with approximately 10.2 molecules of tightly bound water for DPPC and 7.2 for DMPC.[10] Our results for the DMPC–DPPC mixture (50 : 50) highlight this difference. Indeed, due to the difference in the tail size, the lipid membrane exhibits regions with protuberances, as shown in the cartoon of Fig. 4, where the surface of the corresponding head-groups exposed to water is larger in DPPC than that in DMPC. Therefore, only a small quantity of water molecules is released at the beginning of the evaporation process. They constitute the bulk (free) water. Afterwards, the process

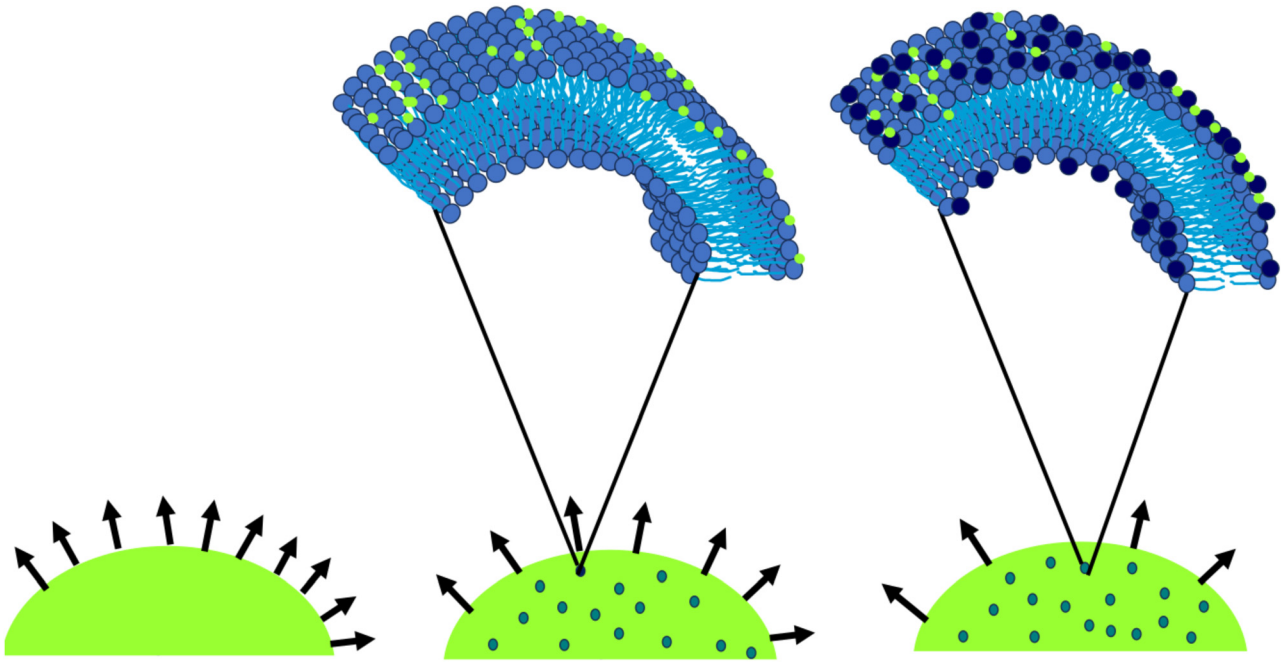

Fig. 4 Schematic picture of two different liposomes: pure (DMPC) and a mixture (DMPC–DPPC), 50 : 50, after the phase transition (liquid or disordered). Since the size of the lipid tails is not the same for the mixture, the hydration area around the polar heads is larger for DPPC lipids (16C, T_m = 42 °C) than that for DMPC (14C, T_m = 24 °C). Consequently, the dehydration process is completely different for the mixture with respect to the pure liposome.

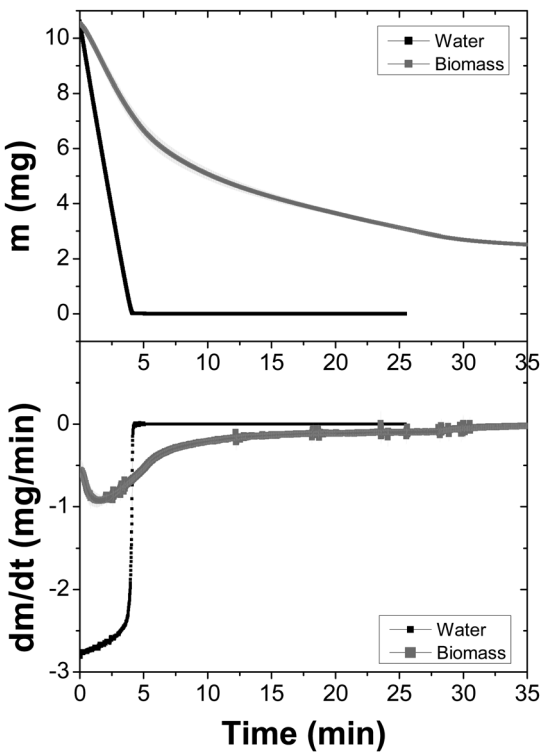

Fig. 5 Dynamics of the dehydration of a *E. coli* biomass measured at 37 °C with a constant helium flux (60 mL min^{-1}). The average and standard deviations of three experiments (due to the fact that the measurements provide many data, the errors bars form a band) are shown. Top: Weight loss as a function of time. Bottom: The first derivative of the data as a function of time. A sample of Milli-Q water is plotted as the reference.

is slower and slower, accounting by the evaporation of hydration water.

Fig. 5 shows the dehydration process of *E. coli* biomass performed at 37 °C. It can be observed that, despite the time of the evaporation event and the asymptotic remaining mass are different, there is a notable similarity between this dynamic and that of the DMPC–DPPC mixture. We will come back later to explain, in a detailed form (Fig. 3 and 5).

As previously mentioned, we evaluated the water loss of little suspension drops of liposomes at temperatures above their phase transitions.[19] Before discussing the evaporation process for these cases, it is important to describe the physical mechanisms behind the phenomenon. Usually, evaporation and condensation are mechanisms that occurs simultaneously, according to the Hertz–Knudsen–Schrage equation,[2,3] which determines the net mass flow rate:

$$\frac{dm_{net}}{dt} = \frac{2}{2 - C_c}\left(\frac{M}{2\pi R}\right)^{1/2}\left[C_c\frac{P_v}{T_v^{1/2}} - C_v\frac{P_l}{T_l^{1/2}}\right], \quad (1)$$

where C_c and C_v are the condensation and evaporation coefficients, respectively, M is the mass per mole, R is the universal gas constant, and P and T are the pressure and temperature for liquid and vapour (subscripts l and v), respectively. In this regard, evaporation involves complicated dynamics where some molecules leave, and others enter in the sample. In order to simplify the process, in the present study, our experiments were carried out using a gas flux. This implies that all the molecules released from the sample are carried away by the gas, and then, the condensation coefficient is null and C_v is the

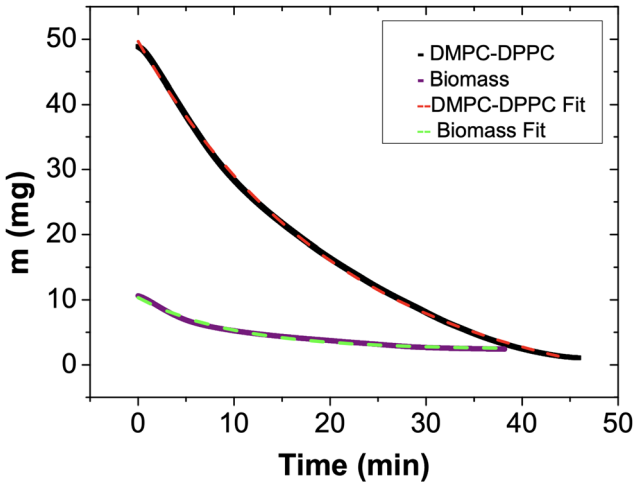

Fig. 6 Weight loss as a function of time (continuous line) and the fitting (dashed line) in representative cases of DMPC–DPPC and biomass. The samples were measured at 37 °C with a constant helium flux (60 mL min^{-1}). See the text for details.

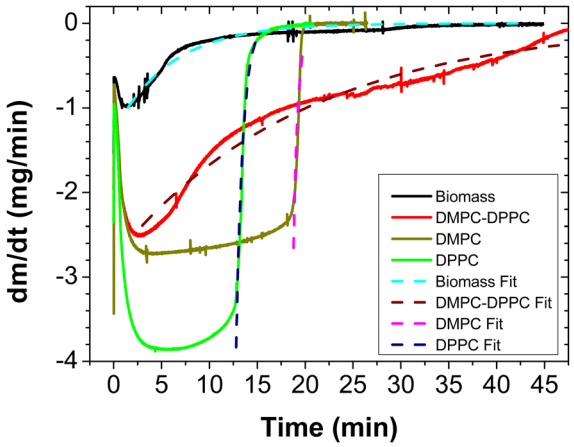

Fig. 7 First derivative (continuous line) of the mass loss as a function of time and the fitting (dashed symbols) for DMPC, DPPC, DMPC–DPPC (50 : 50) liposomes and biomass. All the samples were measured at 37 °C, except DPPC (at 47 °C) with a constant helium flux (60 mL min^{-1}). The volume of the samples was 50 μL and the concentration was 2%.

unity. Therefore, the last equation takes a simpler form:

$$\frac{dm_{net}}{dt} = -\left(\frac{M}{2\pi R}\right)^{1/2}\left[\frac{P_l}{T_l^{1/2}}\right]. \quad (2)$$

or,

$$\frac{dm_{net}}{dt} = -AP_l, \quad (3)$$

where

$$A = -\left(\frac{M}{2\pi R T_l}\right)^{1/2}. \quad (4)$$

The negative sign implies, of course, that there is always a mass loss from the beginning to the end. Except at the very end of the evaporation, eqn (2) perfectly describes the constant mass loss of pure water (black lines), as observed in Fig. 1–3 and 5.

In eqn (3), P_l is the inner pressure exerted by water molecules on the air–water interface. Since there is bulk or free, and bound water, we conceive P_l to be constant for bulk water and proportional to mass for bound water, this one due to the electrostatic interaction with the head-groups of lipids. In the case of this pressure, P_l is then:

$$P_l = Cm_{net}. \quad (5)$$

Employing eqn (3) and (4), we obtain:

$$\frac{dm_{net}}{dt} = -ACm_{net}. \quad (6)$$

Integrating, we obtain

$$m_{net} = m_{net_0}e^{-\mu(t-t_0)}, \quad (7)$$

where $\mu = AC$. We can see t_0 as the time when free water is completely disappeared and bound water starts to evaporate following an exponential decay, where m_{net_0} is the amount of bound water.

In Fig. 6, we depict the mass loss for the DMPC–DPPC liposomes and biomass, fitted by eqn 7. Since the mass loss curves dm_{net}/dt give clearer details of the transition from the bulk to bound water, we show in Fig. 7 the experimental derivatives fitted by the derivative of eqn (7), where μ is a sensitive parameter to describe the evaporation of bound water. Indeed, for suspensions of pure liposomes (DMPC and DPPC), μ is larger than one (2.11 and 1.41, respectively) and for suspensions of hybrid liposomes and biomass, μ is smaller than one (0.05 and 0.07, respectively).

Lipids have different electric dipoles that are located at the beginning of the tails (carbonyls) and the polar head-groups. The latter is the strongest, oriented from the phosphate group (PO_4) to the choline group.[20–22] It should be noted that the phosphate group is a kosmotrope anion, and its small size and high charge density lead to an intense binding of the immediate water molecules.[23,24] Moreover, since its negative charge density is greater than the positive one of the choline group, the PO_4 group is able to orient the contiguous water molecules. They constitute a hydration shell, as recently observed by Saak *et al.*[24,25] Meanwhile, the carbonyl region is the second hydration center in the lipids, because a small amount of water molecules penetrates in this zone following a complex dynamics, as seen in X-ray studies.[12,14,26]

On the other hand, the *E. coli* membrane is a more complex system.[27] It is composed of different phospholipids (phosphatidylethanolamine, PE (57.5%), phosphatidylglycerol, PG (15.1%), cardiolipin, CA (9.8%) and unknown (17.6%) phospholipids), where PE is a zwitterionic lipid, and PG and CA are negatively charged. This gives place to a different interaction compared to the liposomes. While in the liposome case, the interaction of water is with the dipolar head of the lipids, in the cell, there are charged lipids, and therefore the electrostatic interaction is enhanced. Additionally, this *E. coli* strain has approximately 1600 proteins in its membrane.[28] Such proteins are composed of amino acids with charged side chains that

strongly interact with water.[9] Thus, the release process of free water in *E. coli* is shorter than that in the liposome case and the residual mass is larger (at the working temperatures, some water may not evaporate at all).

4 Conclusions

Water equilibrium within a cell is decisive for its appropriate functioning. Studying the dehydration process in a cell membrane allows a better understanding of such equilibrium. While in prior studies, cell dehydration was commonly analysed under osmotic stress conditions, in the present work, this process was simplified by removing the contribution of water condensation. In other words, in a restricted condensing environment (achieved by a gas flux), water–lipid interactions have been investigated in order to understand water permeation and packing. In this context, several experimental methods have been used: microturbidimetry, nuclear magnetic resonances, differential scanning calorimetry, neutron scattering, X-ray spectroscopy, and Fourier transform infrared spectroscopy.[29–31] We analysed the evaporation dynamics of lipid membrane models (DMPC, DPPC and DMPC–DPPC (50 : 50)). We found that evaporation depends on the location of water molecules in the membrane. Such behaviour is driven by the electrostatic interaction between water molecules and the lipid head-groups, and this is clearly observed during the dehydration of the liposomes. Our experimental and theoretical findings, using a very simple model, allow us to understand the non-osmotic dehydration phenomenon of a real cell membrane.

Author contributions

G. H. G. carried out all the experiments. H. M.-U. designed the research and wrote the paper.

Conflicts of interest

There are no conflicts to declare.

Acknowledgements

This work was supported by the CONAHCYT, Mexico (Grant A1-S-8125). We thank C. Ruiz for his insightful comments. G. H. G. acknowledges a scholarship from the CONAHCYT, Mexico.

References

1 Y. Li, K. Konstantopoulos, R. Zhao, Y. Mori and S. X. Sun, *J. Cell Sci.*, 2020, **133**, jcs240341.
2 I. Eames, N. Marr and H. Sabir, *Int. J. Heat Mass Transfer*, 1997, **40**, 2963–2973.
3 R. Marek and J. Straub, *Int. J. Heat Mass Transfer*, 2001, **44**, 39–53.
4 J. H. Crowe, L. M. Crowe, J. F. Carpenter and C. A. Wistrom, *Biochem. J.*, 1987, **242**, 1–10.
5 M. B. França, A. D. Panek and E. Eleutherio, *Comp. Biochem. Physiol., Part A: Mol. Integr. Physiol.*, 2007, **146**, 621–631.
6 S. J. Prestrelski, N. Tedeschi, T. Arakawa and J. F. Carpenter, *Biophys. J.*, 1993, **65**, 661–671.
7 E. Fardelli, M. Lucidi, M. Di Gioacchino, S. Bashiri, L. Persichetti, G. Capecchi, T. Gasperi, A. Sodo, P. Visca and G. Capellini, *Biochim. Biophys. Acta, Biomembr.*, 1864, **2022**, 184045.
8 M. Palaiokostas, W. Ding, G. Shahane and M. Orsi, *Soft Matter*, 2018, **14**, 8496–8508.
9 N. Kučerka, J. Gallová and D. Uhrková, *Chem. Phys. Lipids*, 2019, **221**, 140–144.
10 E. A. Disalvo, *Membrane hydration: the role of water in the structure and function of biological membranes*, Springer, 2015, vol. 71.
11 G. L. Jendrasiak, *J. Nutr. Biochem.*, 1996, **7**, 599–609.
12 E. A. Disalvo, F. Lairion, F. Martini, E. Tymczyszyn, M. Fras, H. Almaleck and G. J. Gordillo, *Biochim. Biophys. Acta, Biomembr.*, 1778, **2008**, 2655–2670.
13 R. M. Lynden-Bell, S. C. Morris and J. D. Barrow, *Water and life: the unique properties of H20*, 2011.
14 M. Chattopadhyay, E. Krok, H. Orlikowska, P. Schwille, H. G. Franquelim and L. Piatkowski, *J. Am. Chem. Soc.*, 2021, **143**, 14551–14562.
15 P. Ball, *Chem. Rev.*, 2008, **108**, 74–108.
16 A. Aksan, A. Hubel and J. C. Bischof, *J. Biomech. Eng.*, 2009, **131**, 074004.
17 M. Jansen and A. Blume, *Biophys. J.*, 1995, **68**, 997–1008.
18 J. C. Mathai, S. Tristram-Nagle, J. F. Nagle and M. L. Zeidel, *J. Gen. Physiol.*, 2008, **131**, 69–76.
19 E. Oropeza-Guzman and J. C. Ruiz-Suárez, *Langmuir*, 2018, **34**, 6869–6873.
20 K. Gawrisch, D. Ruston, J. Zimmerberg, V. Parsegian, R. Rand and N. Fuller, *Biophys. J.*, 1992, **61**, 1213–1223.
21 P. B. Moore, C. F. Lopez and M. L. Klein, *Biophys. J.*, 2001, **81**, 2484–2494.
22 S. Diaz, F. Amalfa, A. Biondi de Lopez and E. Disalvo, *Langmuir*, 1999, **15**, 5179–5182.
23 K. D. Collins, *Biophys. J.*, 1997, **72**, 65–76.
24 L. B. Dreier, A. Wolde-Kidan, D. J. Bonthuis, R. R. Netz, E. H. Backus and M. Bonn, *J. Phys. Chem. Lett.*, 2019, **10**, 6355–6359.
25 C.-M. Saak, L. Dreier, K. Machel, M. Bonn and E. H. Backus, *Faraday Discuss.*, 2023, DOI: **10.1039/D3FD00117B**.
26 S. Simon and T. McIntosh, *Methods in enzymology*, Elsevier, 1986, vol. 127, pp. 511–521.
27 P. M. Oliver, J. A. Crooks, M. Leidl, E. J. Yoon, A. Saghatelian and D. B. Weibel, *J. Bacteriol.*, 2014, **196**, 3386–3398.
28 A. Sueki, F. Stein, M. M. Savitski, J. Selkrig and A. Typas, *Msystems*, 2020, **5**, e00808–e00819.
29 A. Carruthers and D. Melchior, *Biochemistry*, 1983, **22**, 5797–5807.
30 B. Ladbrooke, R. M. Williams and D. Chapman, *Biochim. Biophys. Acta, Biomembr.*, 1968, **150**, 333–340.
31 H. I. Petrache, N. Gouliaev, S. Tristram-Nagle, R. Zhang, R. M. Suter and J. F. Nagle, *Phys. Rev. E: Stat. Phys., Plasmas, Fluids, Relat. Interdiscip. Top.*, 1998, **57**, 7014.

